Transport Function of the Renal Type IIa Na^+/P_i Cotransporter Is Codetermined by Residues in Two Opposing Linker Regions

Katja Köhler, Ian C. Forster, Gerti Stange, Jürg Biber, and Heini Murer

Institute of Physiology, University of Zurich, CH-8057, Zurich, Switzerland

ABSTRACT Two highly similar regions in the predicted first intracellular (ICL-1) and third extracellular loop (ECL-3) of the type IIa Na^+/Pi cotransporter (NaPi-IIa) have been shown previously to contain functionally important sites by applying the substituted cysteine accessibility method (SCAM). Incubation in methanethiosulfonate (MTS) reagents of mutants that contain novel cysteines in both loops led to full inhibition of cotransport activity. To elucidate further the role these regions play in defining the transport mechanism, a double mutant (A203C-S460C) was constructed with novel cysteines in each region. The effect of cysteine modification by different MTS reagents on two electrogenic transport modes (leak and cotransport) was investigated. MTSEA (2-aminoethyl MTS hydrobromide) and MTSES (MTS ethylsulfonate) led to full inhibition of cotransport and increased the leak, whereas incubation in MTSET (2-[trimethylammonium]ethyl MTS bromide) inhibited only cotransport. The behavior of other double mutants with a cysteine retained at one site and hydrophobic or hydrophilic residues substituted at the other site, indicated that most likely only Cys-460 was modifiable, but the residue at Ala-203 was critical for conferring the leak and cotransport mode behavior. Substrate interaction with the double mutant was unaffected by MTS exposure as the apparent P_i and Na^+ affinities for P_i-induced currents and respective activation functions were unchanged after cysteine modification. This suggested that the modified site did not interfere with substrate recognition/binding, but prevents translocation of the fully loaded carrier. The time-dependency of cotransport loss and leak growth during modification of the double cysteine mutant was reciprocal, which suggested that the modified site is a kinetic codeterminant of both transport modes. The behavior is consistent with a kinetic model for NaPi-IIa that predicts mutual exclusiveness of both transport modes. Together, these findings suggest that parts of the opposing linker regions are associated with the NaPi-IIa transport pathway.

KEY WORDS: structure function • electrophysiology • cysteine mutagenesis • P_i-cotransport • leak current

INTRODUCTION

Renal proximal tubular reabsorption of inorganic phosphate is achieved by a secondary active electrogenic Na^+-coupled cotransport process that is mainly mediated by the type IIa Na^+/P_i cotransporter (NaPi-IIa) in the brush border membrane of the proximal tubule (for review see Murer et al., 2000). After expression in *Xenopus* oocytes, the kinetic properties of the NaPi-IIa protein have been described in detail by studying the uptake of $^{32}P_i$ or measurement of the P_i-induced inward current under voltage clamp conditions (Busch et al., 1994; Forster et al., 1997, 1998, 1999). NaPi-IIa exhibits two electrogenic transport modes that can be assayed by electrophysiology: a uniport or leak mode in the absence of external P_i (stoichiometry = 1 Na^+) that can be quantified by using the competitive inhibitor phosphonoformic acid (PFA),* and a cotransport mode (stoichiometry = 3 Na^+: 1 HPO_4^{2-}) (Forster et al., 1999).

The rat NaPi-IIa isoform is a 637 amino acid glycoprotein with a molecular mass of 90–100 kD (Magagnin et al., 1993; for review see Murer et al., 2000). The predicted topological model indicates a secondary structure with eight transmembrane domains, a large extracellular loop with two N-glycosylation sites, and intracellular NH_2 and COOH termini (Magagnin et al., 1993; Hayes et al., 1994; Lambert et al., 1999b). Two highly similar regions in the first intracellular loop (ICL-1) and third extracellular loop (ECL-3) of the protein have been shown to contain functionally important sites (Lambert et al., 1999a, 2001; Kohler et al., 2002) (Fig. 1). Modification of novel cysteines with methanethiosulfonate (MTS) reagents in both loops led to full inhibition of NaPi-IIa–mediated cotransport activity. Moreover, we have established that NaPi-IIa is a functional monomer (Kohler et al., 2000) so that with one HPO_4^{2-} molecule translocated per transport cycle (Busch et al., 1994; Forster et al., 1998, 1999), there is most likely a single P_i translocation pathway per NaPi-IIa protein. As modification of residues in either ICL-1

Address correspondence to Ian C. Forster, Physiologisches Institut, Universität Zürich-Irchel Winterthurerstrasse 190, CH-8057 Zürich, Switzerland. Fax: (41) 1-635-5715; E-mail: IForster@access.unizh.ch

*Abbreviations used in this paper: ECL-3, third extracellular loop; ICL-1, first intracellular loop; MTS, methanethiosulfonate, MTSEA, 2-aminoethyl MTS hydrobromide; MTSET, 2-(triethylammonium) ethyl MTS bromide; NaPi-IIa, type IIa sodium phosphate cotransporter; PFA, phosphonoformic acid; P_i, inorganic phosphate; SCAM, substituted cysteine accessibility method; TMD, transmembrane domain; WT, wild-type.

or ECL-3 leads to a complete loss of cotransport activity, this would suggest that both regions contribute, at least in part, to a common P_i transport pathway. Therefore, we proposed that the P_i transport pathway through NaPi-IIa could be established from the reentrancy of ECL-3 and ICL-1 as part of an aqueous pore (Kohler et al., 2002).

The consensus kinetic scheme for NaPi-IIa and some other Na^+-driven cotransport systems is an alternating access model that incorporates two transport cycles for the leak and cotransport modes (e.g., Parent et al., 1992; Chen et al., 1997; Eskandari et al., 1997; Forster et al., 1998; Yao and Pajor, 2000). Implicit in this scheme is the mutual exclusiveness of the two transport modes: i.e., the leak mode is inoperative during cotransport and vice versa, although it has been difficult to establish this experimentally. This model also provides no insight into the nature of the translocation pathways, for example, whether the cosubstrate cation is translocated via a separate pathway from the driven substrate or both substrates share the same common pathway, as discussed by Sonders and Amara (1996) (see also Su et al., 1996). As mutations in the ICL-1 and ECL-3 linkers of NaPi-IIa also lead to changes in the leak kinetics (Lambert et al., 2001; Kohler et al., 2002), these regions may be candidates not only to associate and form the P_i transport pathway, but may also be involved in the translocation of the cosubstrate cation in the leak mode.

To elucidate further the role of both regions in determining the properties of each transport mode, we constructed a double mutant where cysteines were introduced into ICL-1 and ECL-3 at sites shown previously to be functionally important (Lambert et al., 1999a, 2001; Kohler et al., 2002). When expressed in *Xenopus* oocytes and assayed electrophysiologically using the two-electrode voltage clamp, this mutant (A203C-S460C) displayed essentially WT-like cotransport properties, but a significantly increased leak. External application of different MTS reagents not only led to a complete loss of cotransport function in all cases, but for two reagents (MTSEA, MTSES) the leak increased even further. This effect most likely depended on the size covalently linked moiety. Substitution of other residues individually at these sites indicated that modification of Cys-460 alone occurs in the double mutant, but the opposing residue at Ala-203 was critical for conferring the observed transport properties and may sterically interact with site Ser-460. Finally, the time dependency of the loss of cotransport and the increase in leak during MTS incubation was found to be complementary, supporting the notion that the modified sites interact with conformations associated with both transport modes. These new findings provide evidence that parts of ICL-1 and ECL-3 act as kinetic codeterminants of the uniport and cotransport modes of NaPi-IIa.

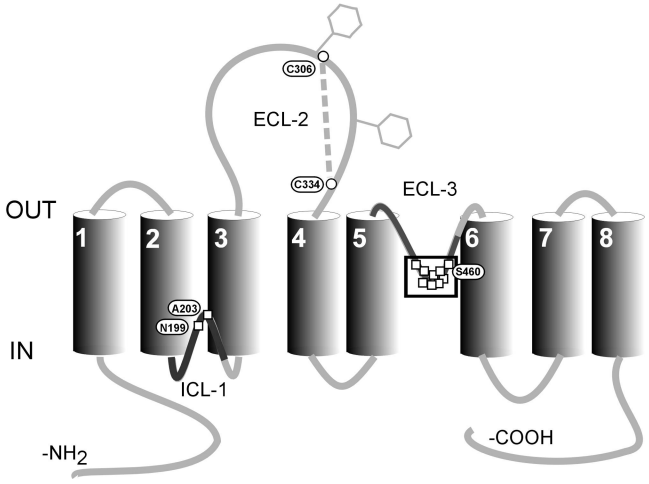

FIGURE 1. Secondary topology of NaPi-IIa showing the eight putative transmembrane domains based on hydrophobicity analysis and topology studies. Two N-glycosylation sites in the second extracellular loop are indicated by hexagons and a cysteine bridge has been identified between Cys-306 and Cys-334. Squares indicate sites where cysteine substitution and/or exposure to MTS reagents alter transport function. The boxed residues in ECL-3 represent a region that forms a proposed 2.5 turn α-helix (Lambert et al., 2001). The bold regions of ICL-1 and ECL-3 represent two stretches of ~50 amino acids that show high similarity (Kohler et al., 2002).

MATERIALS AND METHODS

Reagents and Chemicals

All restriction enzymes were obtained from Amersham Biosciences or Promega. Oligonucleotide primers were obtained from Microsynth and the mutagenesis kit was purchased from Stratagene. MTS (methanethiosulfonate) reagents (MTSEA, 2-aminoethyl MTS hydrobromide; MTSES, sodium (2-sulfonatoethyl)MTS sulfonate; MTSET, 2-(trimethylammonium)ethyl MTS bromide; and MTSEA-biotin, N-biotinylaminoethyl MTS) were obtained from Toronto Research Chemicals. Other reagents were obtained from Fluka.

Molecular Biology

Mutations were introduced after the Quickchange site-directed mutagenesis kit manual (Stratagene) In brief, 10 ng of the plasmid containing the rat NaPi-IIa cDNA were amplified with 2.5 U PfuTurbo (Stratagene) DNA polymerase in the presence of 250 nM primers. PCR amplification was performed with 20 cycles of 95°C (30 s), 55°C (91 min), and 68°C (14 min). Next, 1 U of DpnI were added directly to the reaction and the sample was incubated for 1 h at 37°C to digest the parental DNA. XL1-blue supercompetent cells were transformed with 1 μl reaction mixture and plated onto LB-ampicillin plates. The sequence was verified by sequencing. All constructs were cloned in pSport1 (GIBCO BRL). The in vitro synthesis and capping of cRNAs were done following the Ambion MEGAscript TM T7 kit manual. Briefly, 1 μg of the construct previously linearized by NotI was incubated in the presence of 40 U of T7 RNA polymerase (Promega) and Cap Analogue (New England Biolabs, Inc.) at 37°C for 4 h.

Solutions

The solution compositions for the electrophysiological assays are as follows: Control superfusate ND100 contained (in mM) 100 NaCl, 2 KCl, 1.8 $CaCl_2$, 1 $MgCl_2$, 5 HEPES, adjusted to pH 7.4 with Tris. Control superfusate ND0 was as for ND100, but with N-methyl-D-glucamine replacing Na^+, and adjusted to pH 7.4 with HCl. Solutions with intermediate Na^+ concentrations were prepared by mixing ND0 and ND100 in the appropriate proportions. For the substrate test solutions, P_i was added to ND100 from a 1 M K_2HPO_4/KH_2PO_4 stock preadjusted to pH 7.4, and the Na^+/P_i cotransport inhibitor phosphonoformic acid (PFA) was added to ND100 from frozen stock (in H_2O) to yield a final concentration of 3 mM. MTSEA, MTSES, and MTSET were prepared in DMSO, frozen in aliquots at 1 M, and freshly diluted in precooled ND100 (~4°C) from the stock for each oocyte tested to ensure stability of the reagent. The final concentration of DMSO did not exceed 0.2% and DMSO at this concentration was confirmed not to alter the kinetic characteristics of the expressed constructs.

Xenopus Laevis Oocyte Expression

The procedures for oocyte preparation and cRNA injection have been described in detail elsewhere (Werner et al., 1990). Oocytes were injected with either 50 nl of water or 50 nl of water containing 10 ng of cRNA. Oocytes were incubated in modified Barth's solution and the experiments performed 3–4 d after injection. All pooled data were generated with oocytes from at least two different donor frogs.

Transport Assays and Data Analysis

Radiolabeled $^{32}P_i$ uptake. The procedure used for the $^{32}P_i$ uptake assay has been described in detail elsewhere (Werner et al., 1990). $^{32}P_i$ uptake was measured 3 d after injection of oocytes ($n = 8$).

Electrophysiology. The standard two-electrode voltage clamp technique was used as previously described (Forster et al., 1998). The voltage clamp was a laboratory-built system with membrane current measured using a virtual ground bath electrode and with active series resistance compensation to reduce clamp errors. Oocytes were mounted in a small recording chamber (100 μl volume) and continuously superfused (5ml/min) with test solutions precooled to ~20°C. The steady-state response of an oocyte to P_i and PFA was always measured at a holding potential (V_h) of −50 mV in ND100. Data were acquired online using Digidata 1200 hardware and compatible pClamp8 software (Axon instruments, Inc.). Recorded currents were prefiltered at a bandwidth less than twice the sampling rate (typical sampling rate = 2.5 ms/point; 8 pole low-pass filtering at 20 Hz 3dB bandwidth).

For the P_i activation protocol, P_i-induced currents (I_{Pi}) were obtained by subtraction of the response in the ND100 control solution without P_i. The ratio of current induced by 0.1 mM P_i ($I_{Pi}^{0.1Pi}$) and 1.0 mM P_i ($I_{Pi}^{1.0Pi}$) was determined as a P_i activation index. For the Na^+ activation protocol, I_{Pi} was measured relative to the control solution NDX, where X represents the Na^+ concentration (in mM). The Na^+ activation index was determined by comparing the current in response to 1 mM P_i at 50 mM Na^+ (I_{Pi}^{50Na}) and 100 mM Na^+ (I_{Pi}^{100Na}). Apparent substrate affinities for P_i (K_m^{Pi}) and Na^+ (K_m^{Na}) were estimated by fitting the modified Hill equation to the dose response data as described previously (e.g., Forster et al., 1998). The Hill coefficient, n_H was constrained to 1.0 only for fitting the P_i dose response data. The pH dependency of the transporter was determined by measuring the electrogenic response at pH 7.4 ($I_{Pi}^{pH7.4}$) and pH 6.2 ($I_{Pi}^{pH6.2}$) (with 100 mM Na^+ and 1 mM P_i at V_h = 50 mV) and compared the ratio $I_{Pi}^{6.2}/I_{Pi}^{7.4}$ with that of the WT protein. We assumed that 3 mM PFA was sufficient to fully block the leak. A leak index was then obtained by comparing I_{Pi} (1mM P_i) and I_{PFA} (3 mM PFA), measured relative to the baseline holding current and expressing the leak as a fraction of the total electrogenic transport activity ($I_{PFA}/(I_{PFA}\text{-}I_{Pi})$ (Lambert et al., 2001; Kohler et al., 2002).

For the incubation with MTS reagents, freshly prepared MTSEA or MTSET was applied to the chamber by gravity feed via a 0.5 mm diameter cannula positioned near the cell. Reagents were applied in the presence of ND100 solution. Incubation time was 3 min, followed by a 1 min washout period.

Immunoblot of Oocytes Homogenates

Yolk-free homogenates were prepared 3 d after injection (H_2O or cRNA) by lysing three oocytes together with 60 μl of homogenization buffer [1% elugent (Calbiochem) in 100 mM NaCl, 20 mM Tris/HCl, pH 7.6] by pipetting up and down (Turk et al., 1996). Samples were centrifuged at 16,000 *g* for 3 min at room temperature to pellet the yolk protein. 20 μl of the supernatants in 2× loading buffer (4% SDS, 2 mM EDTA, 20% glycerol, 0.19 M Tris/HCl, pH 6.8, 2 mg/ml bromophenol blue) were separated on a SDS-Page gel and proteins were transferred to a nitro-cellulose membrane (Schleicher & Schuell). The membrane was then processed according to standard procedures (Sambrook et al., 1989) using rabbit polyclonal antibodies raised against synthetic peptides from the NH termini of NaPi type IIa. The specificity of the antibody has been demonstrated previously (Custer et al., 1994). Immunoreactive proteins were detected with a chemiluminescence system (Pierce Chemical Co.).

Streptavidin Precipitation of Biotinylated Protein

Groups of eight oocytes that express S460C or the WT protein were incubated for 5 min in 100 μM MTSEA-Biotin. Biotin-streptavidin precipitation was performed as described previously (Hayes et al., 1994). Briefly, after homogenization in 160 μl of homogenization buffer (see immunoblot of oocyte homogenates), a sample for Western blotting was taken and the oocyte homogenate was incubated for 2 h with streptavidin beads and after washing, precipitated proteins were eluted with 2× loading buffer at 95°C for 5 min. Samples were loaded on an SDS-gel and immunoblotted after protein separation.

Immunohistochemistry

The fixation of *Xenopus laevis* oocytes has been described previously (Hayes et al., 1994). Briefly, the oocytes were immersed for 30 min in PBS containing 3% paraformaldehyde. After rinsing in cold PBS, the eggs were frozen onto thin cork slices using liquid nitrogen–cooled liquid propane. Sections of 5 μm were cut at −23°C using a cryomicrotome, and mounted on chromalaum-gelatin–coated glass slides. For immunostaining, after preincubation in PBS containing 3% milk powder and 0.02% Triton X-100, the sections were first incubated overnight with a rabbit anti-NaPi-IIa antibody (Custer et al., 1994) directed against the NH_2-terminus (dilution, 1:500), followed by incubation with a swine anti-rabbit IgG-conjugated fluorescein-isothiocyanate (FITC) secondary antibody (Dakopatts). Double staining of β-actin filaments and NaPi-IIa was achieved by adding Texas red phalloidin (Molecular Probes). Finally, sections were coverslipped using DAKO Glycergel (Dakopatts) plus 2.5% 1,4-diazabicyclo(2.2.2) octane (Sigma-Aldrich) as a fading retardant. Unspecific binding of the secondary antibodies to the oocytes was tested by omitting the primary antibody. All control incubations were negative.

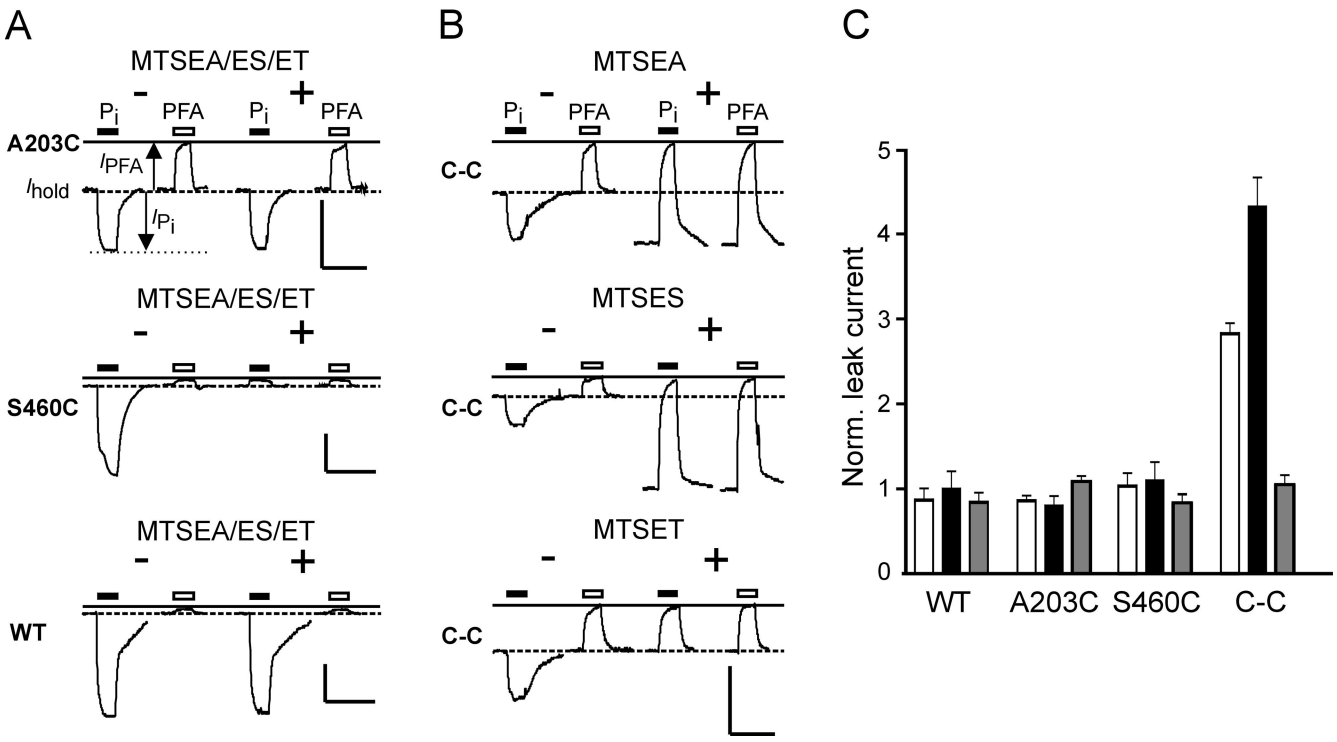

FIGURE 2. Effect of MTS reagents on electrogenic response of C-C mutant. (A) Representative current recordings from oocytes that expressed the single mutants A203C, S460C, and WT NaPi-IIa, before and after incubation in 100 μM MTSEA, MTSES, or MTSET (data shown only for MTSEA as MTSET and MTSES gave similar records). Traces show responses of oocytes to 1 mM P_i (filled bar) and 3 mM PFA (open bar) applied for the period indicated, before (−, left traces) and after (+, right traces) incubation. The continuous line indicates the holding current level reached during the initial PFA application. Dashed line represents holding current (I_{hold}) in ND100 solution. Note that for each cell, the recording baseline levels were not adjusted before and after MTSEA exposure. Note the quantification of transport modes as indicated: substrate-induced currents (I_{PFA}, I_{Pi}) are measured relative to I_{hold}. Uniport or leak activity is then given by $-I_{PFA}$ and the cotransport activity is given by $I_{Pi} - I_{PFA}$. We assume that these substrate concentrations are sufficient to inhibit fully the leak current and that both transport modes are mutually exclusive. Bars: vertical, 50 nA; horizontal, 20 s. (B) Recordings from oocytes expressing the double mutant A203C-S460C (C-C) before (−, left traces) and after (+, right traces) incubation for 3 min with 100 μM MTSEA, MTSES, or MTSES. Note that for the double mutant, the leak current increases only in the presence of MTSEA and MTSES. Bars: vertical, 50 nA; horizontal, 20 s. (C) Pooled data for the leak for oocytes expressing WT, A203C, S460C, and C-C mutant after incubation with MTSEA (white bars), MTSES (black bars), or MTSET (gray bars). Each data point represents mean of five oocytes, normalized to the value before MTS exposure.

RESULTS

Characterization of A203C-S460C Double Mutant

After cRNA injection of *Xenopus* oocytes, the double cysteine mutant (A203C-S460C or C-C[1]) was characterized in terms of protein expression (Western blot) and transport function by measuring the P_i induced current (I_{Pi}) under voltage clamp conditions. The C-C mutant was expressed in comparable amounts and showed a similar expression pattern to the WT NaPi-IIa protein (see Fig. 4 B). Its two electrogenic transport modes (leak and cotransport) were quantified by measuring the response relative to the holding current in ND100 of the same oocyte to applications of saturating concentrations of PFA (3 mM) (I_{PFA}) and P_i (1 mM) (I_{Pi}), respectively (see Fig. 2 A). The leak and cotransport currents are then given, respectively, by $-I_{PFA}$ and I_{Pi}–I_{PFA} (Lambert et al., 2001). The response of the C-C mutant to 1 mM P_i was 30–40% of the WT activity, whereas the PFA-induced response was significantly larger compared with a WT oocyte from the same batch (Fig. 2 B). To take account of different expression levels, the leak current was normalized with respect to the cotransport current, to give a leak index ($I_{PFA}/(I_{PFA} - I_{Pi})$ as described previously (Lambert et al., 2001; Kohler et al., 2002). The C-C mutant showed a sixfold larger leak index (0.51± 0.05, $n = 8$) compared with the WT NaPi-IIa (0.08 ± 0.01) and this was also significantly higher than the value reported previously for the single mutant A203C (0.34 ± 0.06, $n = 6$; Kohler et al., 2002).

As Cys mutagenesis by itself may alter other transport properties of NaPi-IIa as shown previously for mutants

[1]Double mutants were designated with a two-letter nomenclature using the single letter code for amino acids, where the first letter refers to the substituted residue at site Ala-203 and the second letter is the substituted residue at site Ser-460.

in ECL-3 and ICL-1 of NaPi-IIa (Lambert et al., 2001; Kohler et al., 2002), we investigated cotransport mode characteristics such as P_i and Na^+ activation and pH dependency for the C-C mutant and compared them to the WT behavior. Using indices for P_i and Na^+ activation as described previously (Lambert et al., 2001; see MATERIALS AND METHODS), the C-C mutant yielded values ($I_{Pi}^{0.1P_i}/I_{Pi}^{1.0Pi} = 0.47 \pm 0.04$, $I_{Pi}^{50Na}/I_{Pi}^{100Na} = 0.50 \pm 0.06$; $n = 4$) that were within the WT range ($I_{Pi}^{0.1Pi}/I_{Pi}^{1.0Pi} = 0.48 \pm 0.03$; $I_{Pi}^{50Na}/I_{Pi}^{100Na} = 0.47 \pm 0.04$; $n = 4$). Similarly, this mutant was also tested for pH dependency, another hallmark of the type IIa Na^+/P_i cotransporter kinetics. Here the pH-index ($I_{Pi}^{pH6.2}/I_{Pi}^{pH7.4}$) was 0.62 ± 0.07; $n = 4$, which was also comparable to the WT Na-Pi-IIa (0.51 ± 0.06; $n = 4$). These basic steady-state kinetic findings indicated that apart from the leak mode behavior, the cotransport properties, including apparent substrate affinities (at V_h =–50 mV), were unaltered by the cysteine substitutions.

Effect of MTS Reagents on Leak and Cotransport Function

To assess the effect of MTS reagents on transport function, both the uniport and cotransport mode activities were quantitated before and after application of the reagent by measuring the response to PFA (3 mM) and P_i (1 mM), respectively. Three MTS reagents were used: MTSEA, a positively charged reagent (at pH 7.4) that is known to be membrane permeable (Holmgren et al., 1996), MTSET (positively charged), and MTSES (negatively charged), both of which are considered membrane impermeant.

Previously, we established that cotransport activity of mutant S460C was fully abolished by incubation with 100 μM concentrations of MTSEA and MTSET (Lambert et al., 1999a, 2001) for exposure times <5 min. Therefore, the effect of 100 μM MTSEA, MTSET, and MTSES was tested on the transport modes of the C-C mutant as well as the WT and single mutants A203C and S460C as controls expressed in oocytes from the same donor frogs. We assumed that a change in either the P_i or PFA-induced electrogenic responses was evidence for the association of the modified site with the respective transport pathway.

Fig. 2, A and B, illustrate the behavior of representative oocytes that expressed the four constructs before and after incubation with MTSEA, MTSES, or MTSET (100 μM). None of the reagents had a significant effect on the WT or A203C electrogenic responses (Fig. 2 A, top and bottom), whereas for S460C (Fig. 2 A, center), exposure to all three reagents resulted in full inhibition of cotransport mode with no change in the PFA-sensitive current, as reported previously (Lambert et al., 1999a). The C-C mutant also showed the same phenotype with respect to the loss of cotransport mode for all three reagents (Fig. 2 B), but in contrast to the single mutant S460C, the effects on the PFA sensitive current for the C-C mutant depended on the reagent. Only incubation with MTSEA or MTSES led to an increase in leak current (Fig. 2 B). This effect was observed neither for the WT nor for the two single mutants, in agreement with our previous results (Lambert et al., 2001; Kohler et al., 2002). However, after exposure to MTSET, the leak of the C-C mutant remained unchanged. The effect of the different MTS reagents is summarized in Fig. 2 C, which shows the leak after MTS exposure normalized to the leak before MTS exposure, pooled from data from two donor frogs ($n = 5$). Incubation with MTSEA led to two- to threefold gain in leak, whereas MTSES induced an even greater leak increase (up to fivefold). Extending the incubation period or using higher concentrations of MTS reagents did not lead to further change in the PFA-sensitive current (unpublished data). As MTSET appeared to have only a partial effect on the transport properties, cells that had been already exposed to MTSET were reincubated in MTSEA. However, no further change in behavior was observed (unpublished data).

Apparent Na^+ and P_i Affinities Unchanged by Modification

Like the C-C mutant, single Cys mutants that show suppressed cotransport activity after MTS exposure, possess a common electrogenic phenotype whereby the P_i response closely resembles the PFA response (Fig. 2). For the single mutants in ICL-1 and ECL-3, we have concluded previously from this behavior that MTS modification appears to leave the leak mode and substrate recognition intact (P_i or PFA), but subsequent transitions in the cotransport cycle are blocked (Lambert et al., 1999a; Kohler et al., 2002). However, in these studies the substrate-induced currents after MTS treatment were too small for further reliable quantification to test this hypothesis. In the present case, the large leak current of the C-C mutant after Cys-modification allowed us to perform dose responses for P_i activation (at 100 mM Na^+) and Na^+ activation (at 1 mM P_i) before and after incubation with MTSEA to determine whether Cys modification of mutant C-C had changed the apparent substrate affinities. P_i-induced currents were measured at different P_i concentrations before and after incubation with MTSEA (in the presence of 100 mM Na^+) on the same oocyte relative to the holding current in 0 mM P_i, and the values were then normalized to the I_{Pi}^{max} predicted by fitting the modified Hill equation to the data (Fig. 3 A). The apparent affinity for P_i ($K_m^{P_i}$) before (0.056 ± 0.01 mM, $n = 4$)) and after (0.058 ± 0.01 mM, $n = 4$) modification was unchanged and did not differ from $K_m^{P_i}$ for the WT NaPi-IIa (0.061 ± 0.01 mM, $n = 4$). The same was found for the Na^+ activation (in response to 1 mM P_i), where the apparent Na^+ affinities (K_m^{Na}) before (52 ± 8 mM, $n =$

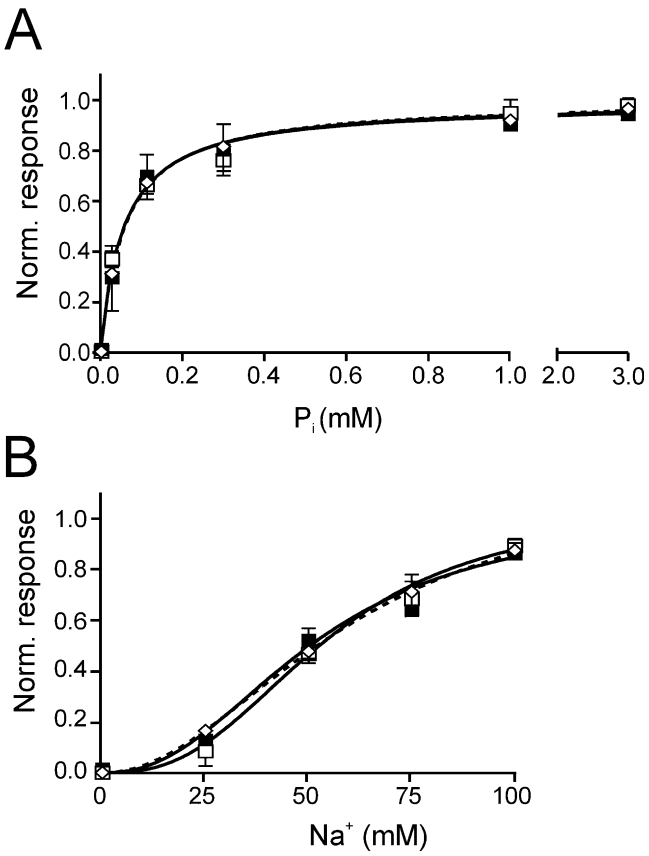

FIGURE 3. Substrate dose responses for C-C mutant and WT before and after modification with MTSEA. (A) P_i activation for WT (open diamonds) and C-C mutant (filled squares) before modification with MTSEA at $V_h = -50$ mV, measured in ND100 with P_i as variable substrate. For the C-C mutant, data are also shown after incubation with MTSEA (open squares), by measuring the change in holding current induced by P_i relative to the holding current in 0 mM P_i. Each data point represents mean ± SEM ($n = 4$). The modified Hill equation was fit to the data to give: $K_m^{Pi} = 0.06 \pm 0.010$ (C-C, −MTSEA); $K_m^{Pi} = 0.06 \pm 0.01$ (C-C, +MTSEA) and $K_m^{Pi} = 0.060 \pm 0.01$ (WT), n_H was constrained to 1.0 for fit. (B) Na^+ activation for WT (open diamonds) and C-C mutant (filled squares) before modification with MTSEA at $V_h = -50$ mV measured at 1 mM P_i with Na^+ as variable substrate. For the C-C mutant, data are also shown after incubation with MTSEA (open squares) by measuring the change in holding current induced by P_i relative to the current in 0 mM P_i. Data were pooled as in A ($n = 4$); fit of Hill equation gave: $K_m^{Na} = 52 \pm 8$ (C-C, −MTSEA), $K_m^{Na} = 55 \pm 6$ (C-C, +MTSEA), $K_m^{Na} = 61 \pm 10$ (WT), $n_H = 2.3$, 2.7, and 2.1, respectively. Points without error bars have SEMs smaller than the symbol size.

4) and after (55 ± 6 mM, $n = 4$) incubation with MTSEA were close to that of the WT NaPi-IIa (61 ± 10 mM, $n = 4$) (Fig. 3 B). Moreover, the form of the activation kinetics, Michaelian for P_i and sigmoidal for Na^+ (i.e., with Hill coefficient, $n_H > 1$), was preserved after MTSEA treatment. These findings strongly suggested that the Cys modification did not prevent the substrate interaction with the protein.

TABLE I

Summary of Mutant Behavior

Protein	Residue at 203	Residue at 460	Transport function: Leak	Transport function: Cotransport	Surface expression
WT	A	S	+	+	+
Single	**C**	S	+	+	+
Double	**C**	**C**	+	+	+
	C	**A**	+	+	+
	C	**L**	+	+	+
	C	**E**	−	−	−
	C	**R**	+	−	+
Single	A	**C**	+	+	+
Double	**S**	**C**	+	+	+
	L	**C**	−	−	+
	R	**C**	−	−	+
	E	**C**	−	−	+

Summary of properties of mutants compared to the WT NaPi-IIa protein. Bold letters indicate the novel residue substituted at indicated site, using the single letter amino acid code. Symbols: +, detectable; −, undetectable.

Characterization of Other Double Mutants

Do both cysteines within the double mutant have to be present to cause the MTS-induced effect on the leak mode of mutant C-C? We attempted to answer this question by constructing other double mutants wherein one of the cysteines at either Ala-203 or Ser-460 was retained and a noncysteine substitution (Ala, Ser, or Leu) made at the other site. These four mutants were designated: S-C, L-C, C-A, and C-L. Furthermore, we attempted to mimic the effect of modification of one cysteine at either Ala-203 or Ser-460 in the C-C mutant by substituting a positively charged Arg with approximately the same molecular size as Cys-MTSEA (mutants R-C, C-R) or a negatively charged Glu, to mimic Cys-MTSES (mutants E-C, C-E). Table I summarizes the functional and expression properties of these mutants, together with the single mutants (A203C, S460C) and WT.

After expression in oocytes, the functionality of all mutants was assayed in $^{32}P_i$ uptake studies. As shown in Fig. 4 A, only mutants S-C, C-A, and C-L showed statistically significant $^{32}P_i$ uptakes above water injected controls. The active mutants S-C and C-A were tested under voltage clamp conditions for their kinetic properties such as P_i and Na^+ activation, leak, and pH dependency. For mutant C-L, only very small P_i induced currents (typically less than −10 nA) could be obtained under voltage clamp conditions, which precluded further kinetic characterization of this mutant. Na^+ and P_i activation and pH dependency for mutants S-C and C-A were within the range obtained for the WT protein ($I_{Pi}^{0.1P_i}/I_{Pi}^{1.0P_i} = 0.6 \pm 0.04$, 0.45 ± 0.04; $I_{Pi}^{50Na}/I_{Pi}^{100Na} = 0.59 \pm 0.05$, 0.56 ± 0.07, $I_{Pi}^{pH6.2}/I_{Pi}^{pH7.4} = 0.39 \pm 0.09$,

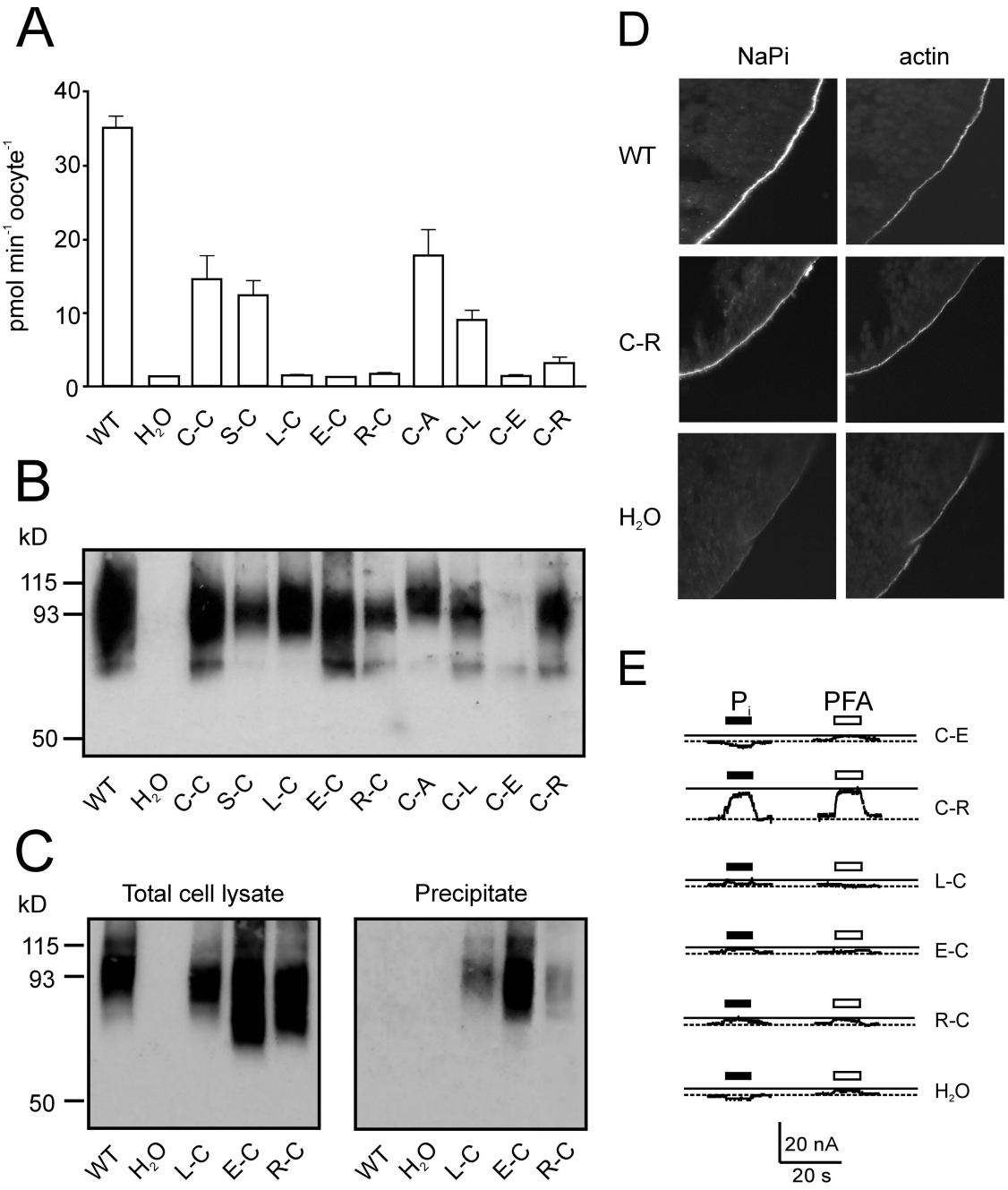

FIGURE 4. Characterization of other double mutants. (A) $^{32}P_i$ uptake of cells injected with WT and mutant cRNA and water-injected oocytes. The bars represent the mean ± SEM ($n = 8$). Only the WT, C-C, S-C, C-A, and C-L mutants gave statistically significant $^{32}P_i$ uptake compared with control oocytes (Students t test, $P < 0.05$). (B) Protein expression of mutants in oocytes. Western blot of whole cell lysate from a pool of 5 oocytes injected with cRNA coding for the indicated mutants as well as the wild-type (WT) and water-injected oocytes as controls. NaPi-IIa was visualized using an antibody raised against the rat NaPi-IIa -NH_2 terminus. (C) Surface biotinylation of mutant constructs. Western blot obtained from a pool of eight oocytes injected either with water, WT or the indicated mutants cRNA. 5 μl of whole oocyte lysate (left) or 15 μl of streptavidin-precipitate of MTSEA-biotinylated oocytes expressing the indicated mutants or WT and water injected oocytes (right). Band at 93 kD confirms that the labeled protein is NaPi-IIa. (D) Immunocytochemical detection of WT NaPi-IIa and C-C mutant and β-actin in cryosections of *Xenopus* oocytes. Oocytes injected with H_2O, or cRNA for WT, or C-C mutant were cut and cryosections labeled with a rabbit polyclonal antibodies directed against the NH_2 terminus of NaPi-IIa and with phalloidin-Texas red. Specific immunostaining appears in the oocyte surface as indicated by the actin signal. No specific NaPi-IIa staining was seen for H_2O injected oocytes. Magnification, 60×. (E) Representative electrogenic response to 1 mM P_i and 3 mM PFA for double mutants. Traces show P_i and PFA-induced currents obtained from oocytes expressing the mutated constructs, measured at 1 mM P_i (filled bar) or 3 mM PFA (open bar) in ND100 and $V_h = -50$ mV. Test substrates were applied for 20 s during period indicated by bars.

0.59 ± 0.12, respectively, $n = 3$), whereas the leak index for both mutants was increased compared with that of the WT. For the C-A mutant this matched that found previously for the A203C single mutant (0.34 ± 0.06, Kohler et al., 2002) and that for the S-C mutant was in agreement with the leak index for the S460C single mutant (0.17 ± 0.02; Lambert et al., 2001). Both indices were smaller than that for the C-C mutant, which suggested that the increase in leak for the double mutant is a cumulative effect of both single Cys mutations.

The lack of function of the other double mutants (E-C, R-C, L-C, C-E, C-R) could be simply due to a lack of expression or a lack of proper targeting to the oocyte membrane. Therefore, expression of the nonfunctional mutants was assessed in Western blot and surface expression of those mutants was determined. As shown in Fig. 4 B, most mutants showed a main band at 80–100 kD and were expressed in amounts comparable to the WT protein, whereas mutant C-E was always only poorly expressed. As the expression pattern of the nonfunctional mutants was identical to the WT NaPi-IIa protein (Fig. 4 B), we investigated the surface expression of these mutants either after biotinylation with MTSEA-Biotin and streptavidin precipitation, or by immunofluorescence. MTSEA-biotinylation has been used previously to detect surface expression of mutant S460C (Lambert et al., 1999a) and is based on the accessibility of this residue with MTSEA. Therefore, mutants containing Cys-460 should be surface biotinylated with MTSEA-biotin and precipitated by streptavidin. Oocytes expressing WT, L-C, E-C, and R-C constructs were incubated with 100 μM MTSEA-Biotin and after streptavidin precipitation (see MATERIALS AND METHODS), labeled proteins were visualized by Western blot using an antibody against the NH_2 terminus of NaPi-IIa. Fig. 4 C (left) shows Western blots of total oocyte lysate of the mutants before streptavidin precipitation. Comparable levels of the glycosylated forms of WT and mutants L-C, E-C, and R-C were observed at 80–100 kD. As indicated in Fig. 4 C (right), after incubation in MTSEA-Biotin, mutants L-C, E-C, and R-C could be precipitated by streptavidin, whereas the WT protein is not labeled by MTSEA and thus could not be precipitated, as expected. This indicates that those mutants (L-C, E-C, R-C) are expressed on the oocyte surface, but are functionally inactive.

Mutant C-R could not be precipitated with streptavidin (unpublished data), which indicated that MTSEA could not bind to this mutant under our experimental conditions. This is consistent with the observation that the single mutant A203C is not inhibited by MTSEA (Kohler et al., 2002). This indicates that this residue is not accessible by the reagent, at least not in the concentration used in this assay (100 μM). Therefore, to establish surface expression of this mutant, we performed immunohistochemistry on sections of oocytes expressing WT and the C-R mutant. Oocyte sections were stained with an NH_2-terminal antibody against NaPi-IIa. The same sections were also stained with phalloidin to visualize actin as a marker of the oocyte membrane. As shown in Fig. 4 D, labeling of WT and C-R resulted in a bright immunofluorescence staining at the oocyte surface that was identical with the actin signal. In H_2O-injected oocytes, no significant NaPi-IIa–specific staining was observed. Therefore, we conclude that mutant C-R was also targeted properly to the oocyte membrane.

From previous studies it is known that mutants can be nonfunctional in terms of mediating $^{32}P_i$ uptake, but they can still operate in the leak mode (Kohler et al., 2002). Therefore, all the nonfunctional double mutants were also tested under electrophysiological conditions for their response to P_i (cotransport mode) and PFA (leak mode). As shown in Fig. 4 E, mutants L-C, E-C, R-C, and C-E showed P_i or PFA-induced currents that were comparable to the typical endogenous responses to these substrates observed in noninjected oocytes from the same donor frog. This indicated that these mutants most likely do not function in either transport mode, despite being properly expressed at the oocyte membrane. On the other hand, mutant C-R consistently showed a significant P_i-induced apparent outward current that was similar to that obtained with PFA (Fig. 4 E). This finding suggested that for this mutant the cotransport mode was inhibited, consistent with its statistically insignificant $^{32}P_i$ uptake compared with C-C, S-C, C-A, and C-L constructs (Fig. 4 A) and the leak mode was still intact. Both substrates, P_i and Na^+, can still bind to the protein, but P_i was not transported. This behavior is consistent with that of mutant S460C after incubation with MTSEA (Fig. 2 A), and suggested that mutation S460R mimicked the electrogenic phenotype that results from modification of Ser-460 by MTSEA or MTSET. However, this mutant showed a PFA-sensitive current similar to that of S460C, which would suggest that this mutant mimics only the modification of site Cys-460 and not the C-C mutant phenotype. Incubation of this mutant with MTSEA did not lead to an increase in leak (unpublished data).

To define further the role both cysteines play in leak mode, the functional mutants S-C and C-A were tested for their response to P_i and PFA before and after incubation with MTSEA, MTSES, and MTSET. As shown in Fig. 5, all three reagents inhibited the P_i-induced current of the S-C mutant, but like the single mutant S460C, none of them led to an increase in leak current observed for the C-C mutant. For the C-A mutant, the P_i as well as the PFA-induced current was unchanged after incubation with MTS reagents, which is in agreement with the data obtained for the A203C single mutant (Fig. 2 A). As we were unable to reproduce the C-C

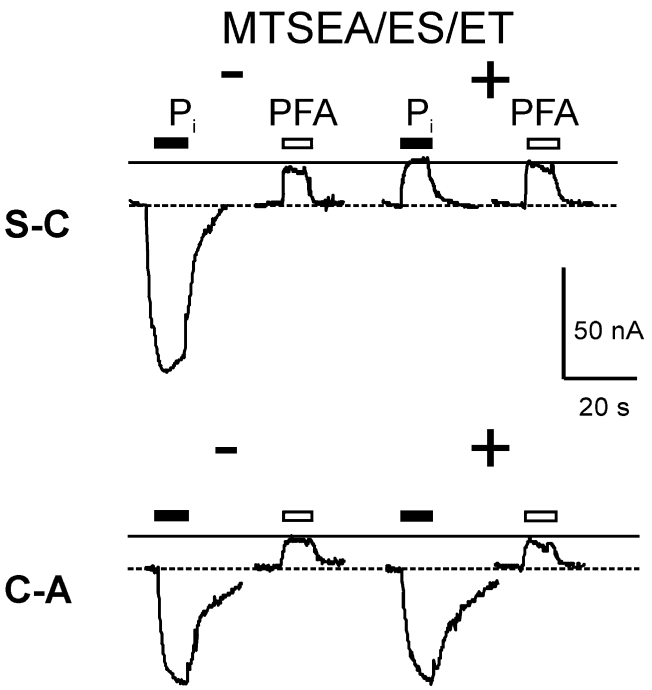

FIGURE 5. Effect of MTS reagents on electrogenic response of functional double mutants with single novel Cys. Representative current recordings from oocytes that expressed S-C and C-A mutants before (−, left traces) and after (+, right traces) incubation for 3 min with 10 μM MTSEA, MTSES, or MTSET (data shown for MTSEA). Each oocyte was tested with 1 mM P_i (filled bar) and 3 mM PFA (open bar) for the period indicated. The continuous line indicates level reached during the initial PFA application. Dashed line represents baseline current in ND100 solution. Note that for each cell, the recording baseline levels were not adjusted before and after MTSEA exposure.

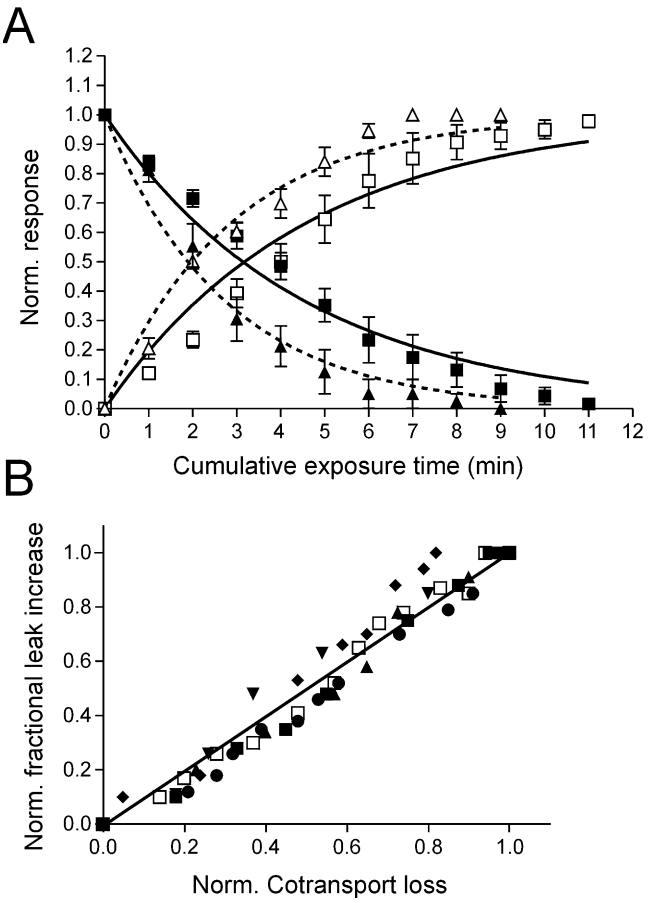

FIGURE 6. Quantification of cysteine modification reaction in terms of cotransport loss and leak gain. (A) Loss of cotransport function (filled symbols) and gain in leak (open symbols) for C-C mutant. Oocytes expressing the mutant were incubated for the indicated cumulative time with a fixed concentration (5 μM) of MTSEA (squares) or MTSES (triangles) and the electrogenic response to 1 mM P_i (cotransport mode) and 3 mM PFA (leak mode) was measured. The transport activity was normalized as explained in the text. Continuous (MTSEA) and dotted (MTSES) lines are fits to the data with a single exponential function of the form: $\exp(-[\text{MTS}]\ t\ k)$, for normalized cotransport loss, or: $1 - \exp(-[\text{MTS}]\ t\ k)$, for normalized fractional leak gain, where [MTS] is the concentration of MTS reagent (in μM), t is the cumulated exposure time (s) and k is the effective second order rate constant ($\mu M^{-1}\ s^{-1}$). Each data point represents mean ± SEM (n = 6). Points without error bars have SEMs smaller than symbol size. (B) Isochronic plot of normalized cotransport loss and fractional, normalized leak gain for the same cells as in A, for the MTSEA exposure. Each symbol represents a different oocyte.

leak phenotype with any other substitutions, we concluded that a Cys residue at each site seems to be required to increase the PFA-sensitive current.

Reciprocity of Transport Mode Modification

Cysteine modification by MTS reagents can be described by second order reaction kinetics (e.g., Karlin and Akabas, 1998). The time (or concentration) dependency of altered transport function can be used to yield an estimate of the effective reaction (modification) rate constant, as we have described previously for single mutants in ICL-1 and ECL-3 (Lambert et al., 2001; Kohler et al., 2002). For the C-C mutant, MTSEA and MTSES led to changes in two transport processes that could be independently quantitated from the respective response to P_i and PFA during the time course of the reaction. We determined the effective second-order reaction rate constant (k) for the modification of each transport mode, using the cumulative exposure time as a variable with a fixed concentration of MTSEA (5 μM) or MTSES (5 μM) (Fig. 6 A). To compare the two reactions among oocytes with different expression levels, we normalized the cotransport activity at a given cumulative exposure time (t) to the initial cotransport activity (i.e., $[I_{PFA} - I_{Pi}]/[I^0_{PFA} - I^0_{Pi}]$). The gain in leak was expressed as the change in I_{PFA} for a given t, relative to the initial PFA response (I^0_{PFA}) and normalized to the change determined at the end of the reaction (I^∞_{PFA}), i.e., $(I_{PFA} - I^0_{PFA})/(I^\infty_{PFA} - I^0_{PFA})$. The data were fit with exponential decay (cotransport loss) or exponential growth (leak gain) functions respectively, to estimate a pseudo first order

rate constant (k') for the MTSEA/ES-Cys reactions, from which we obtained k ($= k'/[\text{MTSEA/ES}]$). An obvious reciprocity in the time course of the two reactions is seen (Fig. 6 A) and k for the change in each transport mode was very similar ($k = 7.2 \times 10^{-4}$ s^{-1} μM^{-1} (cotransport loss); $k = 7.3 \times 10^{-4}$ s^{-1} μM^{-1} [leak gain]). For MTSES the same reciprocal relation was observed but the estimated reaction rate constants were somewhat larger than those for MTSEA ($k = 1.2 \times 10^{-3}$ s^{-1} μM^{-1} [cotransport loss]; 1.10^{-3} s^{-1} μM^{-1} [leak gain]).

As Fig. 6 A shows, the pooled time dependency data did, however, deviate slightly from the model predictions for a single exponential process. This might reflect experimental variations among individual oocytes, e.g., variability in time of exposure to MTS reagents, or invalidity of the Cys modification model. An alternative representation of these data, which ameliorates these uncertainties by eliminating the time as a variable, is the isochronic plot (Fig. 6 B). If the cotransport loss and leak gain follow the same time course (independent of expression level and the specific form of the reaction function), we would expect the points to lie on a straight line. As depicted in Fig. 6 B, the isochronic plot the dataset for each oocyte confirms this prediction and strongly supports the idea that the modification of the two transport modes is reciprocal.

For mutant S-C, the dose dependency for MTSEA-induced cotransport loss was more similar than that for mutant C-C with $k = 7.6 \times 10^{-4}$ s^{-1} μM^{-1}, whereas even after a long incubation time, no significant increase in leak was observed for this mutant (unpublished data).

DISCUSSION

We have previously identified functionally important sites in two highly similar linker regions (ICL-1, ECL-3) of NaPi-IIa by means of SCAM (Lambert et al., 1999a, 2001; Kohler et al., 2002). Transport inhibition by MTS reagents for novel cysteines in both regions follows a similar pattern: after MTS modification, cotransport is inhibited, but the leak mode still operates. Moreover, as we have previously established that the NaPi-IIa protein behaves as a functional monomer (Kohler et al., 2000), with the given stoichiometry of 1 HPO_4^{2-} for the cotransport cycle (Forster et al., 1999), a single cotransport pathway per NaPi-IIa protein is implied. We therefore proposed that since modification of the novel Cys residues in both linkers by MTS reagents leads to a full loss of cotransport function, a physical and functional association of these regions could contribute to a common P_i transport pathway through NaPi-IIa (Kohler et al., 2002).

Evidence for ICL-1–ECL-3 Interaction—Codetermination of Transport Mode

The introduction of a novel cysteine into each putative linker region of NaPi-IIa involves relatively conservative substitutions (Ser-Cys at 460 and Ala-Cys at 203) that are reflected in the retention of WT-like cotransport mode behavior (apparent substrate activation affinities, pH dependency) for the C-C mutant, but with a significantly increased PFA-inhibitable leak. Single Cys substitution at either site also results in mutants that show increased leak compared with the WT; however, the effect is not as significant as for the C-C mutant (Lambert et al., 1999a, 2001; Kohler et al., 2002). Therefore, the leak increase appears to be a cumulative effect of each Cys substitution. This behavior suggests that in addition to the previously hypothesized role that ICL-1 and ECL-3 play in codetermining the cotransport mode (Kohler et al., 2002), they are also involved in conferring properties to the NaPi-IIa leak pathway. This notion is further supported by our finding that the leak activity increases significantly after MTEA/ES treatment for the double mutant, but not for the single mutants.

Like other mutants with novel and modifiable cysteines substituted at functionally important sites in ICL-1 (Kohler et al., 2002) and ECL-3 (Lambert et al., 2001), C-C mutant displays a similar phenotype at the end of the Cys-modification reaction, namely that only the leak mode operates and that the P_i and PFA responses appear identical, i.e., the Cys modification appears to uncouple the two transport modes from one another. The large leak of the C-C mutant also allowed us to quantify the time course of the Cys-modification reaction: loss of cotransport function paralleled gain of leak current with close agreement between the estimated reaction rates and strongly correlated time course for each process.

The behavior of the C-C mutant is consistent with the current kinetic scheme for NaPi-IIa (Forster et al., 2002), in which occupancy of states associated with the binding and translocation of substrate (P_i) precludes uniport mode operation and vice versa, as illustrated in Fig. 7. Before Cys-modification (Fig. 7 A), the transport cycle proceeds around one of two loops (uniport [left], or cotransport [right]) that share three common transitions (empty carrier and binding of 1 Na^+ ion). The probability of cycling in the uniport or cotransport mode depends on the presence and concentration of external P_i. Only one binding step involves P_i, thereby resulting in Michaelian-like P_i-activation (Fig. 3 A), whereas the Na^+-activation (Fig. 3 B) is sigmoidal because >1 Na^+ ion interacts with the protein/cycle. In either mode, PFA at sufficiently high concentration can inhibit both cycles by shifting the state occupancy to a blocked state (2*). After Cys modification (Fig. 7 B), uniport activity still occurs that can be similarly blocked by PFA, but now P_i can also progressively inhibit the leak mode by increasing the probability of occupying state three. The leak suppression by P_i would be expected to be Michaelian, as we observe (Fig. 3 A). Moreover, the finding of a sigmoi-

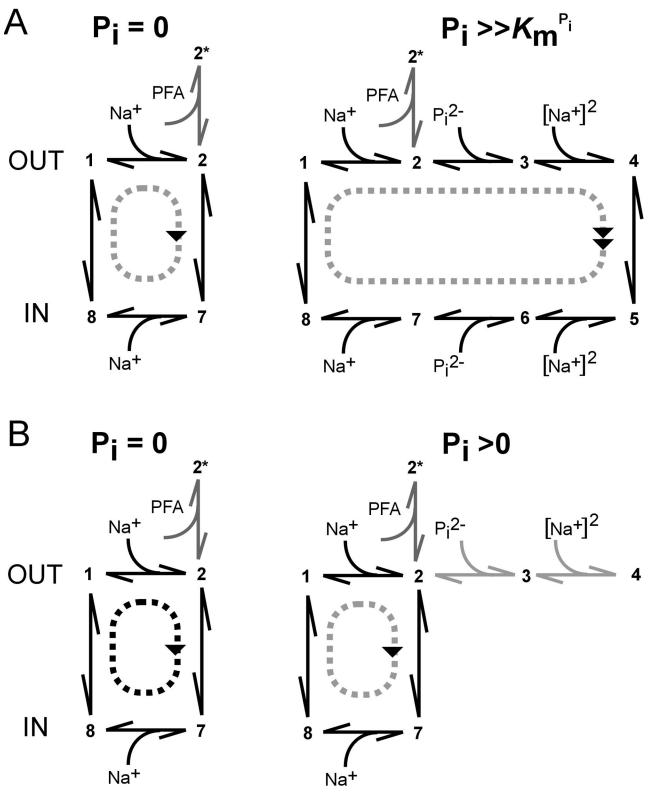

FIGURE 7. Interpreting the effect of MTS reagents on the transport properties of NaPi-IIa, based on an alternating access kinetic scheme. (A) Before Cys modification, transport activity assumes either leak mode (left) or cotransport mode (right), depending on the availability and concentration of external P_i. It is assumed that the internal concentrations of Na^+ and P_i are such that the cycle proceeds in the direction indicated. (B) After Cys-modification, leak mode still operates (left) in the absence of external P_i. In the case of MTSES/MTSEA, a higher turnover rate is also predicted that could result from modification of rates associated with the transition 2–7. For external $P_i > 0$, the probability of occupancy of state 3 increases, thereby reducing the probability of transition 2–7 occurring, so that the leak activity is progressively suppressed in a dose dependent manner as the concentrations of external P_i and/or Na^+ increase (see text). At saturating P_i, and Na^+, the probability of occupying state 4 is high, but the translocation transition (4–5) is prevented by the modified Cys residue.

dal Na^+-activation curve after MTS modification indicates that the system can proceed to state 4 (fully loaded carrier), but the modified Cys prevents the normal translocation to state five. The invariance of the apparent substrate affinities before and after Cys modification and the form of activation (Michaelian or sigmoidal) strongly suggests that the modified Cys is associated with and/or interacts with the translocation pathway itself, rather than with parts of the protein associated with substrate recognition and binding.

Differential Effects of MTS Reagents Sidedness of MTS Reaction

When the C-C mutant was incubated with MTSEA or MTSES, the cotransport activity was completely abolished and the leak increased, whereas incubation in MTSET resulted only in a loss of cotransport function. In contrast, for the single S460C mutant the effects of all three reagents were indistinguishable: invariant leak and suppression of cotransport. As all three reagents induce a loss of cotransport mode for the C-C mutant, independent of the charge of the reagent (MTSET[+]; MTSEA[+]; MTSES[−]), this would suggest that electrostatic effects do not play a role in blocking the cotransport pathway.

On the other hand, our finding that two oppositely charged and membrane-impermeant MTS-modifying reagents (MTSET; MTSES) have a differential effect on the C-C mutant leak might suggest that the charge introduced at the modified site(s) plays a critical role in determining the leak pathway kinetics. Yet, MTSEA, also assumed positively charged at the pH used in our assays, led to the same phenotype as MTSES. One further characteristic that distinguishes these reagents from one another is their effective molecular volumes when covalently linked to a cysteine (MTSEA-Cys = 125 Å^3; MTSES-Cys = 142 Å^3; MTSET-Cys = 173 Å^3; Xu et al., 2000). The larger bulk of MTSET may therefore be the reason for the lack of altered leak. Alternatively, one might postulate that positively charged MTSEA exerts a dual effect due to its slight membrane permeability (Holmgren et al., 1996), whereby it could modify Cys-460 externally to block the cotransport mode and modify Cys-203 internally to increase the leak. This scenario seems unlikely because, at the concentration used for external application (100 μM), we would not expect significant cytosolic accumulation of MTSEA. Together with our previously reported finding that exposure to 10 mM external MTSEA results in only a marginal loss of cotransport function of the single A203C mutant (Kohler et al., 2002), we therefore assume that all the MTS reagents exerted their effect on the C-C mutant from the outside.

Evidence that Only Cys-460 Is Modified

Is the increased leak a result of MTS modification of both cysteines or either one? We were unable to recapitulate the C-C mutant leak phenotype before MTS modification with any of the other double mutants, which indicated that having a cysteine at each site is critical for this behavior. Moreover, mutants with only one Cys present at either site showed no increase in leak after exposure to MTS reagents, which might suggest that modification of both Cys residues is a necessary condition. Nevertheless, the modification of Cys-203 in the C-C mutant would necessitate a significant increase in its accessibility through the presence, or modification of Cys-460. We attempted to mimic this case with the C-R mutant by substituting an Arg at Ser-460 to have a similar molecular volume (122 Å^3) as Cys-

MTSEA (125 Å^3) (Xu et al., 2000). Before MTS exposure, P_i induced the same response as PFA, which indicated that this mutant appears to function only in the leak mode. If modification of Cys-460 alone were responsible for the increased leak in the C-C mutant, we would expect the C-R mutant to display a higher leak than the S460C mutant. However, this appears not to be the case as the P_i/PFA-induced currents were similar to those of the S460C mutant. Moreover, the addition of MTSEA/ES to the C-R mutant did not alter its leak, as would be expected if Cys-203 had become amenable to MTS modification through having a Cys + MTSEA-like residue at Ser-460.

On the other hand, if only Cys-460 were accessible, the altered leak mode of the C-C mutant compared with the single S460C mutant might result from a steric interaction between Cys-203 and Cys-460 + MTS. Support for this is strongly suggested by the behavior of another single mutant in ECL-3, identified in a previous study (Lambert et al., 2001). There we showed that substitution of a cysteine at Ala-453 in ECL-3 resulted in a mutant with an increased leak after MTSEA modification (and concomitant loss of cotransport function), similar to the behavior of the C-C mutant. As Ala-453 is also located in the same stretch of functionally important sites as Ser-460 in ECL-3, one scenario might be that the increased leak turnover for the C-C mutant arises through a steric interaction between the novel Cys-203 in ICL-1 and Cys-460 in ECL-3. Subsequent MTS modification of Cys-460 alone would lead to a construct that mimics the behavior of A453C. We would then predict that the apparent accessibility of Cys-460 in the C-C mutant, as quantified by the effective second order reaction rate constant (k), would also be reduced, since we previously reported an ~10-fold decrease in apparent accessibility of A453C compared with S460C (Lambert et al., 2001). Indeed, k for MTSEA modification of the double mutant (7.2×10^{-4} μM^{-1} s^{-1}) is approximately an order of magnitude smaller than previously reported values for S460C alone (6.37×10^{-3} μM^{-1} s^{-1}) (Lambert et al., 2001) and is comparable with that reported for A453C (6.54×10^{-4} μM^{-1} s^{-1}) from the same study.

Further evidence for a steric effect of Cys-203 on the leak pathway in the C-C mutant comes from the behavior of the other double mutants (Table I). Introducing a cysteine at Ala-203 leads to an increase in leak relative to the cotransport activity even before MTSEA exposure (Kohler et al., 2002), which could be explained by a steric effect of Cys-203 on the transport pathway. Substitution with a Ser is tolerated, leading to a WT-like mutant, whereas introduction of larger hydrophobic (Leu) or charged residues (Glu, Arg) leads to membrane-localized, but nonfunctional mutants. These findings suggest that this is a sterically sensitive site and the introduction of bulky residues here (Leu, Arg, Glu) may induce a significant conformational change that fully disrupts the transport pathway.

That Cys-203 may not be accessible by externally applied MTSEA is also consistent with our finding that the transport activity of the single A203C mutant is only weakly affected by the reagent (Kohler et al., 2002). Although we cannot fully exclude modification of both novel cysteines in the C-C mutant, we would favor a steric interaction of the MTS-inaccessible Cys-203 with the MTS-accessible Cys-460, which also supports our proposition that both loops are closely associated within the protein.

Structure-function Implications: Opposed Reentrant Loops as a Putative Motif for Substrate Translocation

This present study strengthens the case for the role of opposed, reentrant regions to establish a transport pathway through the NaPi-IIa protein and moreover demonstrates that both transport modes are intimately associated with these linker regions. It would be tempting to speculate that both substrate translocation in either mode occurs through the same pathway; however, our findings based on the behavior of the double mutant do not allow us to reach a definitive conclusion in this respect.

Significantly, these two opposing regions are conserved in members of the type IIa Na^+/P_i cotransporter family from eukaryotic systems, including *Caenorhabditis elegans*, as well as the prokaryotic NaPi-IIa homologue from *V. cholerae* (Werner and Kinne, 2001; Forster et al., 2002). This suggests that these repeats may serve a common function in all Na^+-coupled P_i cotransporters. Interestingly, for the Na^+/Ca^{2+} exchanger, opposed stretches of amino acids that are conserved among all members of this family were shown to be functionally important and have been suggested to form the transport pathway of the protein (Schwarz and Benzer, 1997; Philipson and Nicoll, 2000; Qiu et al., 2001). Moreover, opposed reentrant loops that contain residues critical for substrate binding and translocation have been identified in members of the excitatory amino acid transporter family (Grunewald and Kanner, 2000; Slotboom et al., 2001; Brocke et al., 2002). Finally, as predicted by the hourglass model proposed for the AQP-1 water channel, two opposed reentrant loops interact with each other, forming part of the aqueous pathway and participate in selection of neutral from charged solutes (Murata et al., 2000; Jung et al., 1994).

The authors acknowledge financial support from grants to H. Murer from the Swiss National Science Foundation (31-46523), the Fridericus Stiftung, Vaduz, FL-9490; Hartmann Müller-Stiftung (Zurich), the Olga Mayenfisch-Stiftung (Zurich), and the Union Bank of Switzerland (Zurich) (Bu 704/7-1).

Submitted: 12 June 2002
Revised: 10 September 2002
Accepted: 27 September 2002

REFERENCES

Brocke, L., A. Bendahan, M. Grunewald, and B.I. Kanner. 2002. Proximity of two oppositely oriented reentrant loops in the glutamate transporter GLT-1 identified by paired cysteine mutagenesis. *J. Biol. Chem.* 277:3985–3992.

Busch, A., S. Waldegger, T. Herzer, J. Biber, D. Markovich, G. Hayes, H. Murer, and F. Lang. 1994. Electrophysiological analysis of Na^+/P_i cotransport mediated by a transporter cloned from rat kidney and expressed in Xenopus oocytes. *Proc. Natl. Acad. Sci. USA.* 91:8205–8208.

Chen, X.Z., M.J. Coady, F. Jalal, B. Wallendorff, and J.Y. Lapointe. 1997. Sodium leak pathway and substrate binding order in the Na^+-glucose cotransporter. *Biophys. J.* 73:2503–2510.

Custer, M., M. Lotscher, J. Biber, H. Murer, and B. Kaissling. 1994. Expression of Na-P_i cotransport in rat kidney: localization by RT-PCR and immunohistochemistry. *Am. J. Physiol.* 266:F767–F774.

Eskandari, S., D.D. Loo, G. Dai, O. Levy, E.M. Wright, and N. Carrasco. 1997. Thyroid Na^+/I^- symporter. Mechanism, stoichiometry, and specificity. *J. Biol. Chem.* 272:27230–27238.

Forster, I.C., C.A. Wagner, A.E. Busch, F. Lang, J. Biber, N. Hernando, H. Murer, and A. Werner. 1997. Electrophysiological characterization of the flounder type II Na^+/P_i cotransporter (NaPi-5) expressed in *Xenopus laevis* oocytes. *J. Mem. Biol.* 160:9–25.

Forster, I., N. Hernando, J. Biber, and H. Murer. 1998. The voltage dependence of a cloned mammalian renal type II Na^+/P_i cotransporter (NaPi-2). *J. Gen. Physiol.* 112:1–18.

Forster, I., D.D. Loo, and S. Eskandari. 1999. Stoichiometry and Na^+ binding cooperativity of rat and flounder renal type II Na^+/P_i cotransporters. *Am. J. Physiol.* 276:F644–F649.

Forster, I.C., K. Kohler, J. Biber, and H. Murer. 2002. Forging the link between structure and function of electrogenic transporters: the renal type IIa Na^+/P_i cotransporter as a case study. *Prog. Biophys. Mol. Biol.* 80:69–108.

Grunewald, M., and B.I. Kanner. 2000. The accessibility of a novel reentrant loop of the glutamate transporter GLT-1 is restricted by its substrate. *J. Biol. Chem.* 275:9684–9689.

Hayes, G., A. Busch, M. Lotscher, S. Waldegger, F. Lang, F. Verrey, J. Biber, and H. Murer. 1994. Role of N-linked glycosylation in rat renal Na/Pi-cotransport. *J. Biol. Chem.* 269:24143–24149.

Holmgren, M., Y. Liu, Y. Xu, and G. Yellen. 1996. On the use of thiol-modifying agents to determine channel topology. *Neuropharmacology.* 35:797–804.

Jung, J.S., G.M. Preston, B.L. Smith, W.B. Guggino, and P. Agre. 1994. Molecular structure of the water channel through aquaporin CHIP. The hourglass model. *J. Biol. Chem.* 269:14648–14654.

Karlin, A., and M.H. Akabas. 1998. Substituted-cysteine accessibility method. *Methods Enzymol.* 293:123–145.

Kohler, K., I.C. Forster, G. Lambert, J. Biber, and H. Murer. 2000. The functional unit of the renal type IIa Na^+/P_i cotransporter is a monomer. *J. Biol. Chem.* 275:26113–26120.

Kohler, K., I.C. Forster, G. Stange, J. Biber, and H. Murer. 2002. Identification of functionally important sites in the first intracellular loop of the NaPi-IIa cotransporter. *Am. J. Physiol.* 282:F687–696.

Lambert, G., I.C. Forster, G. Stange, J. Biber, and H. Murer. 1999a. Properties of the mutant Ser-460-Cys implicate this site in a functionally important region of the type IIa Na^+/P_i cotransporter protein. *J. Gen. Physiol.* 114:637–652.

Lambert, G., M. Traebert, N. Hernando, J. Biber, and H. Murer. 1999b. Studies on the topology of the renal type II NaPi-cotransporter. *Pflugers Arch.* 437:972–978.

Lambert, G., I.C. Forster, G. Stange, K. Kohler, J. Biber, and H. Murer. 2001. Cysteine mutagenesis reveals novel structure-function features within the predicted third extracellular loop of the type IIa Na^+/P_i cotransporter. *J. Gen. Physiol.* 117:533–546.

Magagnin, S., A. Werner, D. Markovich, V. Sorribas, G. Stange, J. Biber, and H. Murer. 1993. Expression cloning of human and rat renal cortex Na/Pi cotransport. *Proc. Natl. Acad. Sci. USA.* 90: 5979–5983.

Murata, K., K. Mitsuoka, T. Hirai, T. Walz, P. Agre, J.B. Heymann, A. Engel, and Y. Fujiyoshi. 2000. Structural determinants of water permeation through aquaporin-1. *Nature.* 407:599–605.

Murer, H., N. Hernando, I. Forster, and J. Biber. 2000. Proximal tubular phosphate reabsorption: molecular mechanisms. *Physiol. Rev.* 80:1373–1409.

Parent, L., S. Supplisson, D.D. Loo, and E.M. Wright. 1992. Electrogenic properties of the cloned Na^+/glucose cotransporter: II. A transport model under nonrapid equilibrium conditions. *J. Membr. Biol.* 125:63–79.

Philipson, K.D., and D.A. Nicoll. 2000. Sodium-calcium exchange: a molecular perspective. *Annu. Rev. Physiol.* 62:111–133.

Qiu, Z., D.A. Nicoll, and K.D. Philipson. 2001. Helix packing of functionally important regions of the cardiac Na^+-Ca^{2+} exchanger. *J. Biol. Chem.* 276:194–199.

Sambrook, J., E.F. Fritsch, and A.M. Maniatis. 1989. Molecular Cloning: A Laboratory Manual. Cold Spring Harbor Laboratory, Cold Spring Harbor, NY. 18.66–18.75.

Schwarz, E.M., and S. Benzer. 1997. Calx, a Na-Ca exchanger gene of *Drosophila melanogaster. Proc. Natl. Acad. Sci. USA.* 94:10249–10254.

Slotboom, D.J., W.N. Konings, and J.S. Lolkema. 2001. The structure of glutamate transporters shows channel-like features. *FEBS Lett.* 492:183–186.

Sonders, M.S., and S.G. Amara. 1996. Channels in transporters. *Curr. Opin. Neurobiol.* 6:294–302.

Su, A., S. Mager, S.L. Mayo, and H.A. Lester. 1996. A multi-substrate single-file model for ion-coupled transporters. *Biophys. J.* 70:762–777.

Turk, E., C.J. Kerner, M.P. Lostao, and E.M. Wright. 1996. Membrane topology of the human Na^+/glucose cotransporter SGLT1. *J. Biol. Chem.* 271:1925–1934.

Werner, A., J. Biber, J. Forgo, M. Palacin, and H. Murer. 1990. Expression of renal transport systems for inorganic phosphate and sulfate in *Xenopus laevis* oocytes. *J. Biol. Chem.* 265:12331–12336.

Werner, A., and R.K. Kinne. 2001. Evolution of the Na-P_i cotransport systems. *Am. J. Physiol.* 280:R301–R312.

Xu, Y., D.A. Kakhniashvili, D.A. Gremse, D.O. Wood, J.A. Mayor, D.E. Walters, and R.S. Kaplan. 2000. The yeast mitochondrial citrate transport protein. Probing the roles of cysteines, Arg(181), and Arg(189) in transporter function. *J. Biol. Chem.* 275:7117–7124.

Yao, X., and A.M. Pajor. 2000. The transport properties of the human renal Na^+- dicarboxylate cotransporter under voltage-clamp conditions. *Am. J. Physiol.* 279:F54–F64.